01

Luminescence transformation mechanisms of indocyanine green dye in the presence of gold nanorods

© T.S. Kondratenko[1], T.A. Chevychelova[1], O.V. Ovchinnikov[1], M.S. Smirnov[1,2], A.S. Perepelitsa[1]

[1] Voronezh State University,
394018 Voronezh, Russia
[2] Voronezh State University of Engineering Technologies,
394036 Voronezh, Russia

e-mail: optichka@yandex.ru

Received November 17, 2021
Revised December 27, 2021
Accepted December 29, 2021

Spectral-luminescent manifestations of the plasmon-exciton interaction between gold nanorods (Au NRs) with average length and diameter of 35 ± 5 nm and 9 ± 2 nm, passivated by molecules of cetyltrimethylammonium bromide (CTAB) and the indocyanine green dye (ICG) molecules are found. Extinguishing of the ICG luminescence near Au NRs and its buildup are detected at spacial separation of hybrid nanosystem components achieved by a spherical shell of SiO_2 with an average thickness of 26 ± 5 nm formed on the Au NRs. The amplification of the luminescence with growth of the dielectric shell is provided due to blocking of steric transformations of ICG polymethine chain when the interaction emerges between the dye and the silicious shell, and the Purcell effect.

Keywords: luminescence, indocyanine green, gold nanorods, Purcell effect.

DOI: 10.21883/EOS.2022.06.54712.2938-21

Introduction

Currently, the development of stable multifunctional complexes that provide directing and localizing of the existing and luminescent agents *in vivo* is a relevant problem for the diagnostics of oncological diseases [1–3,4]. Complexes based on the indocyanine green (ICG) dye are among promising materials in the field of modern medicine [5–12]. Its absorption and luminescence are within the near IR region (780-910 nm), that coincides with the therapeutic transparency window of the biological tissue [13–20]. This dye is not only able to work as a biomarker in the near IR region, but also can be an agent for photothermal and photodynamic therapy [5–7,11,12]. However, disadvantages of ICG, such as low quantum yield of IR luminescence ($\sim 2.5\%$ in aqueous solution), which is promoted by the mobility of its molecular structure, especially the polymethine chain, low photo- and thermal-stability, impede its biomedical application.

To resolve the above-mentioned problems, a number of ICG stabilization methods are proposed: encapsulation using derivatives of calcium phosphate [21], mesoporous silicon nanoparticles [22], polymer nanocomposites [23], binding with lipid nanoparticles [24,25], molecules of albumine [26,27], nanofibers, quantum dots [28–30], plasmon nanoparticles [12,27,31–36].

Creation of hybrid nanostructures based on luminescent objects and plasmon nanoparticles of silver and gold for different applications of photonics and biomedicine, as well as investigation of their spectral properties are relevant tasks today [12,31–46]. The issues of plasmon nanoparticles field effect on luminescent properties of emitters in plasmon-exciton nanostructures are actively discussed [37–40]. The works discuss techniques to create hybrid nanostructures based on colloidal quantum dots and plasmon nanoparticles, that provide for the manifestation of plasmon-exciton interactions of different types in spectral-luminescent properties. The main problem is to select conditions (distance between components, geometry of nanostructures, setting of resonant frequencies of the emitter and resonator) that provide for effective amplification of the luminescence.

Another type of luminescent objects being extensively investigated are nanostructures of dye molecules of different classes with metal nanoparticles. The effect of metal nanoparticles on dye properties can vary in a very wide range [12,27,31–36,42–46]. Possible effects are a change in type and probability of self-association of the dye, an extinguishing of fluorescence of the dye due to nonradiative transfer of electron excitation, as well as a change in the probability of spontaneous emission due to the Purcell effect [47–49]. Also, a decrease in the number of degrees of freedom and achievement of molecular skeleton rigidity of the molecule at its adsorption on the surface of a plasmon nanoparticle are possible.

There is a number of ICG investigations demonstrated successful use of gold nanoparticles for improvement of ICG properties when it is used as a medical filler [28–36]. These investigations most commonly are focused on the biomedical aspect of the problem [30–36]. The use of created plasmon-exciton nanostructures in the field of biomarking, photothermal and photodynamic therapy and

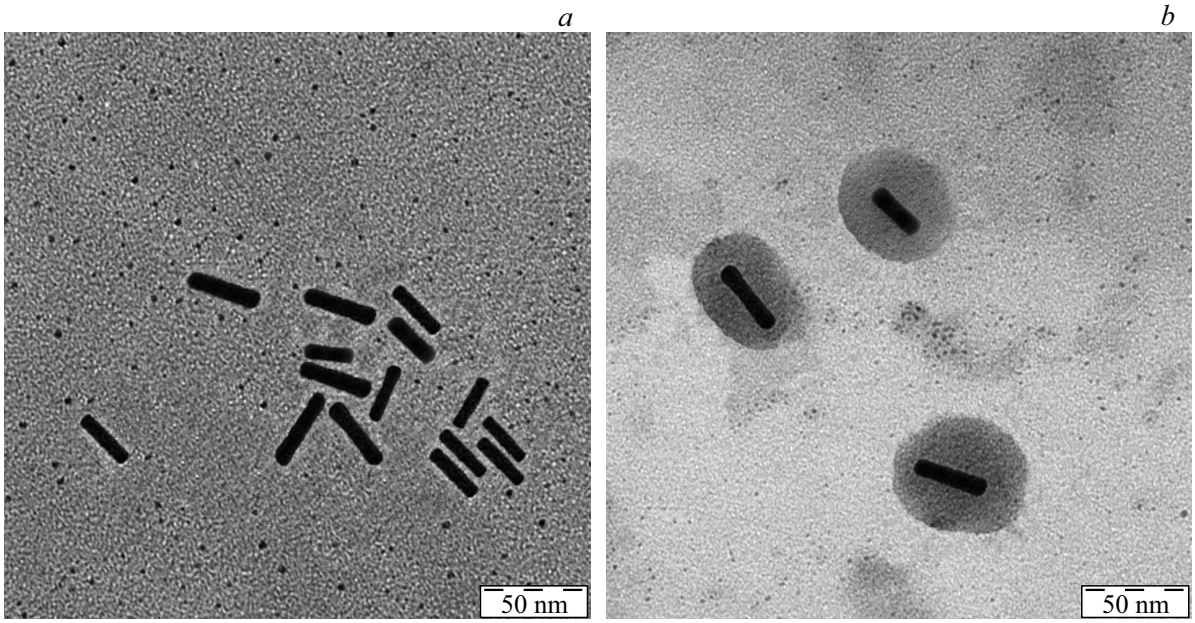

Figure 1. TEM-images of Au NRs (*a*), Au NRs/SiO_2 (*b*).

their cytotoxicity are discussed. Thus, in [34] parameters of optimum configuration of the Au@SiO_2@mSiO_2 nanoplatform are reported that provide almost twofold increase in temperature, a fivefold increase in efficiency of formation of active forms of oxygen and, finally, a threefold increase in the capability of cancer cell neutralization as compared with free molecules of ICG.

In [35] the work of complicated, peptide-functionalized tLyp-1-structures that contain (ICG) mesoporous, silicon dioxide-coated gold nanorods is demonstrated. It is shown that they have a double function, can be used as a fluorescent probe in the near IR region and as an agent of photodynamic therapy aimed at malignant cells.

The conjugation of a dye diluted in the serum albumin HAS with island films of silver nanoparticles composed of silver particle partial coating applied on a glass slide by chemical reduction of silver, or with complex lamellar nanostructures of gold nanospheres/silica/gold nanospheres increases the luminescence from the dye by 20–30 times [33–36].

To successfully use the ICG and structures based on it, a relevant fundamental task is the control of photoprocesses in molecules of the ICG dye that provide optimum IR luminescent properties. However, the existing studies pay no attention to the physical and chemical mechanisms that provide improvement of the parameters of ICG work as a multifunctional medical filler when conjugating molecules with plasmon nanoparticles.

In this study we consider features of manifestations of the plasmon-exciton interaction in ICG dye luminescence spectra and kinetics, which is realized in the case of association with gold nanorods passivated by molecules of CTAB and coated with a spherical dielectric shell of silicon dioxide (SiO_2).

Materials and methods

The investigation is concerned with mixtures of the ICG dye with gold nanorods (Au NRs), as well as Au NRs coated with a dielectric shell of SiO_2 (Au NRs/SiO_2). Plasmon Au NRs were produced by means of colloidal synthesis in the presence of a surface-active agent (SAA) of the cetyltrimethylammonium bromide (CTAB), which serves as a growth coordinator for the gold nanorods [39,40,50]. The procedure to produce Au NRs is a multistage process and consists in successive preparation and mixing of seed and growth solutions. The role of seed solution was played by the solution of spherical nanoparticles of gold, Au NPs (~ 3 nm), obtained as a result of chemical reduction of $HAuCl_4$ (7 μl, 0.36 M) by solution of $NaBH_4$ (1.0 ml, 5 mM) in the presence of CTAB (20 ml, 0.02 mM). The growth solution was obtained as a result of mixing of $HAuCl_4$ (28 μl, 0.36 M), CTAB (50 ml, 0.1 mM) and $C_6H_8O_6$ (5 ml, 0.05 μM). Adding 60 μl of $AgNO_3$ (0.02 M) to the growth solution coordinates the growth of Au NRs.

The structures of Au NRs/SiO_2 were formed within the aqueous technique using (3-mercaptopropyl)trimethoxysilane (3-MPTMS) as a binding agent on the surface of Au NRs and sodium metasilicate ($Na_2O(SiO_2) \cdot 9H_2O$) as a precursor of the main layer of SiO_2 [40].

The obtained colloidal solutions of Au NRs and Au NRs/SiO_2 were stripped of reaction products by multiple centrifuging and repeated dispersing of the residue in distilled water.

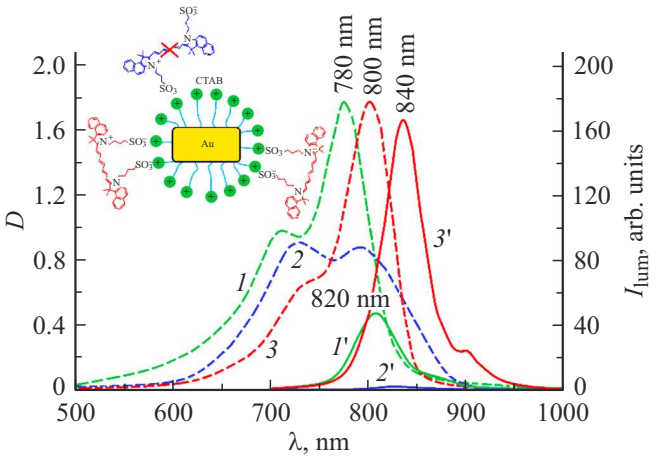

Figure 2. Spectra of light extinction (dashed line) and luminescence (solid line) of the specimens under study: *1, 1′* — ICG in aqueous solution (10^{-5} M); *2, 2′* — ICG + CTAB in a ratio of $\nu_{ICG}/\nu_{CTAB} = 10^2$ m.f.; *3, 3′* — ICG + CTAB in a ratio of $\nu_{ICG}/\nu_{CTAB} = 2 \cdot 10^{-2}$ m.f. In the insert — scheme of coordination of ICG molecules in the presence of CTAB.

Sized and morphology of Au NRs and Au NRs/SiO_2 were determined using a transmission electron microscope (TEM, Libra 120, CarlZeiss, Germany). The analysis of TEM-images has shown that the applied technique makes it possible to obtain Au NRs with average length and diameter of 35 ± 5 nm and 9 ± 2 nm, respectively, while the length-to-diameter ratio of nanorods is 3.8 (Fig. 1). Thickness of the SiO_2 shell on the surface of Au NRs is 26 ± 5 nm (Fig. 1, *b*). Dispersion of Au NRs in ensemble was ~ 30%.

Mixtures of molecules of an organic dye with Au NRs were obtained by introducing the aqueous solution of ICG (10^{-5} M) into the colloidal solution of NRs with the following ratio of the number of dye molecules to the number of gold nanorods $[n(\text{ICG})]:[n(\text{NRs})] = 1{:}50$, 1:100, 1:500, 1:1000, 1:1500.

It is worth noting that molecules of CTAB are not only coordinators of growth for Au NRs, but also possess the micellae-form properties with the possibility of encapsulation of ICG molecules in them. Therefore a dye in aqueous solution of CTAB was considered as of reference for comparison. To form micellae, CTAB was diluted in water in a concentration of $5 \cdot 10^{-2}$ M and heated up to a temperature of 40°C. The ICG encapsulation was performed by introducing the dye aqueous solution into the solution of CTAB with molar ratios of $\nu_{ICG}/\nu_{CTAB} = 10^2$, $2 \cdot 10^{-2}$ m. f. at a temperature of 30°C. This concentration of CTAB is equivalent to the concentration used for the synthesis of Au NRs.

Spectra of optical absorption and luminescence of the prepared specimens were recorded using a USB2000+ spectrophotometer (OceanOptics, USA). The luminescence was excited by a LPC-836 semiconductor pulse laser (Mitsubishi, Japan) at a wavelength of 660 nm with a power of 300 mW.

The kinetics of IR luminescence in the emission band of ICG monomer was investigated using a PicoSingleTCSPC system for time-correlated counting of photons with a InGaAsKIT-IF-25C single-photon detector (MicroPhoton-Devices, Italy) and a PMC-100-20 photomultiplier module with controller (Becker & Hickle). A PICOPOWERLD660 semiconductor pulse laser was used as an excitation source (with a wavelength of 660 nm, a pulse length of 60 ps) (Alphalas, Germany). Time resolution of this setup configuration was 0.12 ns and limited by characteristics of the single-photon detector. ICG luminescence attenuation curves were approximated using deconvolution with experimentally measured response of devices, which allowed controlling the measurement of the luminescence attenuation time with an accuracy of at least 0.05 ns.

Quantum yield of the ICG luminescence was determined by the relative method using the following equation:

$$QY = QY_R \frac{I}{I_R} \frac{D_R}{D} \frac{n^2}{n_R^2}, \quad (1)$$

where QY_R — quantum yield of reference luminescence, I and I_R — integral intensity in luminescence band of sample and reference, D and D_R — absorbances at the excitation wavelength for sample and reference (in the experiments it was ~ 0.1), n and n_R — refraction coefficients of solution with sample and reference, respectively. A solution of ICG dye in DMSO with a quantum yield of 12% in the region of 830 nm was used as the reference for the quantum yield of luminescence in the IR region [51].

The presented results are obtained at a temperature of 300 K.

Experimental results and discussion

Spectra of optical absorption and luminescence of ICG molecules in aqueous solution and CTAB-micellae Due to the possible effect of CTAB on spectral and structural properties of the dye [52], first of all we considered the behavior of ICG spectral properties in its presence. Initial absorption spectrum of the aqueous ICG with a concentration of 10^{-5} M (Fig. 2, curve *1*) is a curve having its maximum in the region of 780 nm, which corresponds to the absorption of ICG monomer, and a local peak in the region of 700 nm, which corresponds to the oscillating structure of $\pi \rightarrow \pi^*$-transition of the monomer [13,18]. In the luminescence spectrum of this solution with the excitation at 660 nm a peak is observed with a maximum at 820 nm, which corresponds to the emission of ICG monomer (Fig. 2, curve *1′*).

When molecules of CTAB are added to the ICG solution, absorption spectra of the dye are transformed significantly. At low concentrations of CTAB molecules in the solution, when about 100 molecules of ICG are accounted for one SAA molecule ($\nu_{ICG}/\nu_{CTAB} = 10^2$ m.f.), the curve of ICG absorption has two peaks at 715 and 800 nm (Fig. 2, curve *2*). The peak at 800 nm corresponds to the absorption

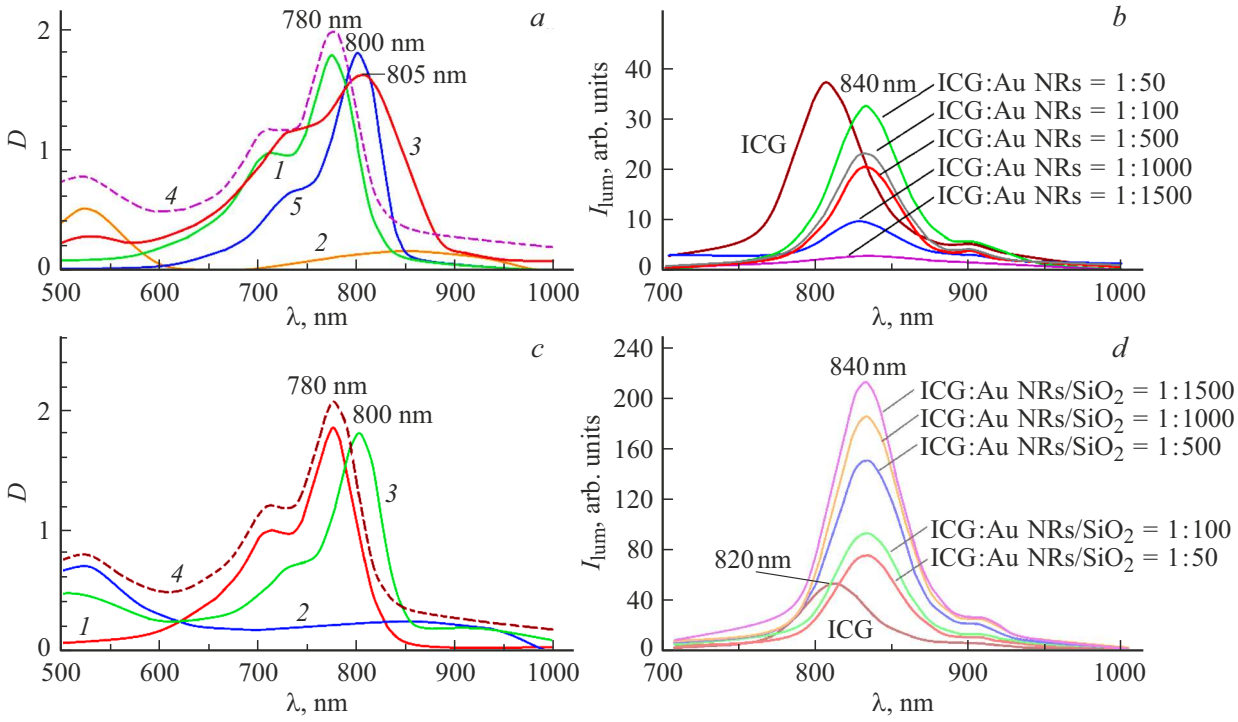

Figure 3. Spectra of absorption (*a, c*) and luminescence (*b, d*) of ICG in mixtures with Au NRs and Au NRs/SiO_2, $\lambda_{excit} = 660$ nm: *1* — ICG in aqueous solution (10^{-5} M), *2* — Au NRs (Au NRs/SiO_2), *3* — Au NRs (Au NRs/SiO_2) + ICG (experimentally obtained spectrum), *4* — sum of spectra of Au NRs (Au NRs/SiO_2) and ICG, ICG + CTAB in a ratio of $\nu_{ICG}/\nu_{CTAB} = 2 \cdot 10^{-2}$ m.f.

band of monomer shifted towards the long-wave region by 20 nm as compared with the peak in the aqueous solution of ICG, while the peak at 710 nm corresponds to light absorption by the dimer form of ICG [13–20]. It is also shifted by 10 nm in relation to the absorption peak of the aqueous solution, containing dimers of ICG. These shifts are caused by the electrostatic interaction of cation CTAB-micellae with negatively charged chromophoric groups of ICG. Thus, at a low concentration of CTAB, the dye assembling to dimers is typical for the solution, which is manifested as a sharp drop of intensity of its light emission (Fig. 2, curve *2′*). It should be noted, that the maximum of luminescence spectra of the ICG monomer with encapsulation in CTAB-micellae (840 nm), as well as the absorption peak, is shifted to the long-wave region as compared with the aqueous solution, which is caused by the interaction of chromophoric groups of the dye with molecules of CTAB.

With increase in concentration of CTAB molecules in the solution ($\nu_{ICG}/\nu_{CTAB} = 2 \cdot 10^{-2}$ m.f.), the absorption spectrum of ICG has maximum absorbance again in the absorption region of dye monomer (800 nm), while intensity of light emission increases by 4 times (Fig. 2, curves *3* and *3′*). The increase in intensity of light emission in case of ICG dye stabilization by CTAB micellae is caused by blocking of steric transformations of the ICG polymethine chain due to the interaction with molecules of CTAB.

Spectra of optical absorption and luminescence of ICG molecules in the presence of gold nanoparticles

Let us consider behavior of spectral properties of the dye in the presence of Au NRs in two different situations: closely located components of the mixture (distance of about the length of a CTAB molecule, 2.5 nm [53]) and located at a distance of about thickness of the SiO_2 shell, 26 ± 5 nm for Au NRs/SiO_2 + ICG (Fig. 3).

In the extinction spectrum of Au NRs we observed two peaks located at 530 and 840 nm, that correspond to transverse and longitudinal dipole modes of the localized plasmon resonance, which is typical for gold nanorods [54] (Fig. 3, *a*, curve *2*). The formation of Au NRs/SiO_2 system results in an increase in scattering over the entire spectral profile. At the same time, the maximum in the region of 840 nm, in essence, does not change its position. The considerable half-width of peaks of the transverse and longitudinal localized plasmon resonances of Au NRs and Au NRs/SiO_2 is caused mainly by the inhomogeneous broadening. Thus, the peak of dipole mode of the localized plasmon resonance lies in the region of light emission of the ICG monomer.

When mixing the aqueous solution of the dye with the solution of Au NRs, the extinction spectra had their maximum in the region of 805 nm, corresponding to absorption of dye monomers, and a shift in relation to the peak position in the aqueous solution, as in the case of

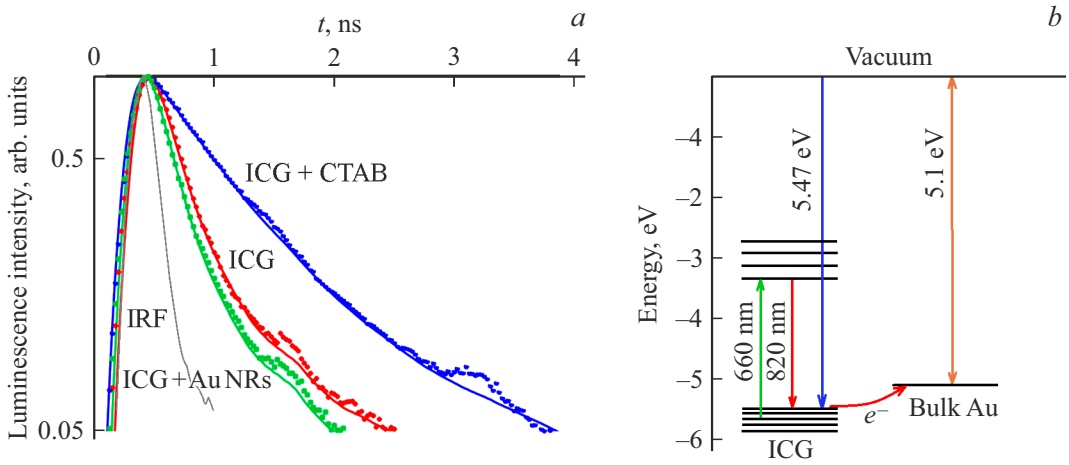

Figure 4. Kinetics of luminescence attenuation (a), scheme of electron excitation transfer in hybrid nanostructures of ICG + Au NRs (b).

CTAB-micellae. However, the profile of extinction spectrum is significantly different from the spectrum of dye in CTAB-micellae and is not a simple sum of extinction spectra of initial components of the mixture (Fig. 3, *a*, curves *3* and *4*), which indicates that the components interact in the solution. The presence of CTAB growth coordinator molecules on the surface of metal nanoparticle probably, as in the case of encapsulation of dye molecules into CTAB-micellae, provides for formation of a structure shown in the insert in Fig. 2 due to the electrostatic interaction of cation CTAB-micellae with negatively charged chromophoric groups of the dye.

When mixing the aqueous solution of the dye with the solution of Au NRs/SiO_2, the extinction spectrum peak corresponding to the absorption of dye monomers is shifted in relation to the peak position in the aqueous solution, as in the case of CTAB-micellae (Fig. 3, *c*). However, in this case molecules of CTAB on the surface of Au NRs are covered by the silicious shell, thus the transformation of the spectrum profile of ICG molecules are caused by the interaction with plasmon Au NRs/SiO_2.

Luminescent properties of the ICG dye in the presence of Au NRs and Au NRs/SiO_2 change in different manner. In the case of mixtures of Au NRs + ICG, in the spectra of luminescence excited by radiation with a wavelength of 660 nm, we observed a shift of the emission maximum towards the long-wave region by 20 nm to 840 nm as compared with the aqueous solution of the dye. At the same time, the light emission extinguished as concentration of Au NRs in the solution increased (Fig. 3, *b*). The observed changes are caused by the charge phototransfer between molecules of the ICG dye and Au NRs. At the same time, the interaction between CTAB and ICG dye with the dye kept in monomer form probably should only increase the intensity of its luminescence (Fig. 3, *a*, curve *3*).

When forming mixtures of Au NRs/SiO_2 with ICG, an increase in intensity of light emission by five times is observed in the luminescence spectra with increase in concentration of Au NRs/SiO_2 in the mixture (Fig. 3, *d*). Quantum yield of the dye luminescence has increased from 3.2% in aqueous solution to 15% in the mixture with Au NRs/SiO_2. In this case the distance between Au NRs/SiO_2 and a dye molecule is defined by the average thickness of the SiO_2 shell.

Two mechanisms of this increase in light emission intensity are possible: blocking of nonradiative processes caused by steric transformations of the ICG polymethine chain due to the interaction with the silicious shell, and amplification in the field of metal nanoparticle acting as a nanoresonator.

Figure 4, *a* shows curves of luminescence attenuation in the emission band of the ICG dye at 840 nm. For the cases of ICG molecules in aqueous solution and in mixture with Au NRs, the curves of attenuation do not differ from each other, i.e. average lifetime of luminescence in the emission band of the ICG monomer remains unchanged (Fig. 4, *a*). Average lifetime of luminescence for ICG in aqueous solution and in mixture with Au NRs was 0.18 ± 0.05 ns. It should be noted, that we determined the average lifetime of luminescence by experimental curves of luminescence attenuation using the following expressions for the approximation:

$$I(t) = \sum_{i=1}^{2} a_i \tau_i, \quad \langle \tau \rangle = \frac{\sum i = 1^2 a_i \tau_i}{\sum_{i=1}^{2} a_i}, \tag{2}$$

where a_i — amplitude and τ_i — the time constant of the i-component in the luminescence attenuation curve. a_i and τ_i values were obtained by approximating the luminescence attenuation curves by the sum of the two exponents:

$$I(t) = \sum_{i=1}^{2} a_i \exp[t/\tau_i]. \tag{3}$$

The presented experimental data indicate that the considerable luminescence extinguishing of the dye monomer

in the presence of Au NRs with unchanged lifetime of the luminescence occurs due to photoinduced charge transfer. Relative positions of HOMO-LUMO-levels of the dye and the Fermi level of gold confirm this possibility (Fig. 4, *c*). The energy of dye photoionization is about 5.47 eV [55]. The energy of the Fermi level for Au — 5.1 eV [56]. The position of HOMO-level of the dye is below the Fermi level for metal and equal to 5.5 eV.

In the case of ICG encapsulation into CTAB-micellae, the monomer luminescence buildup is accompanied by a deceleration of the attenuation kinetics and an increase in the average lifetime of dye luminescence up to 0.56 ns. Thus, molecules of the CTAB growth coordinator used in the synthesis of Au NRs promote coordination of the dye on the surface of nanoparticle, but not significantly contribute to the formation of luminescent properties of the ICG in the presence of Au NRs.

When preparing mixtures of ICG with Au NRs/SiO_2, along with the increase in their quantum yield luminescence, we observed a considerable acceleration of the luminescence attenuation kinetics down to the limit of the experimental setup resolution (about 0.12 ns). Such behavior of luminescent properties indicates the manifestation of the Purcell effect [47–49]. Presumably, creation of structures of the Au NRs/SiO_2 type with a SiO_2 layer thickness of 26 nm breaks the conditions for charge transfer between components of the mixture, and Au NRs/SiO_2 play the role of nanoresonators with oscillation modes close to the frequency of ICG monomer luminescence.

Conclusion

In this study we investigated the effect of Au NRs with an average wavelength and diameter of 35 ± 5 nm and 9 ± 2 nm on luminescent properties of molecules of the organic ICG dye. It is shown that association of ICG molecules with Au NRs results in extinguishing of luminescence in the band of the dye monomer, which can be explained by photoinduced charge transfer between components. In the case of spatial separation of the associate components, due to formation of Au NRs/SiO_2 structures in mixtures with molecules of the ICG dye a 5-time increase in light emission intensity of the dye is observed with simultaneous reduction of luminescence lifetime. These changes are considered as manifestation of the Purcell effect.

0.1. Funding

This study was supported by grant of the President of the Russian Federation № MK-3411.2021.1.2.

Conflict of interest

The authors declare that they have no conflict of interest.

References

[1] M. Ogawa, N. Kosaka, P.L. Choyke, H. Kobayashi. Cancer Res., **69**, 1268 (2007). DOI: 10.1158/0008-5472.can-08-3116
[2] P. Xue, R. Yang, L. Sun, Q. Li, L. Zhang, Zh. Xu, Y. Kang. Nano-Micro Lett., **10** (74), 1 (2018). DOI: 10.1007/s40820-018-0227-z
[3] A.N. Spitsyn, D.V. Utkin, O.S. Kuznetsov, P.S. Yerokhin, N.A. Osina, V.I. Kochubey. Opt. i spektr., **129** (1), 100 (2021) (in Russian). DOI: 10.21883/EOS.2022.06.54712.2938-21
[4] P. Das, A. Sedighi, U.J. Krull. Anal. Chim. Acta, **1041**, 1 (2018). DOI: 10.1016/j.aca.2018.07.060
[5] H.-J. Lim, Ch.-H. Oh. Photodiagnosis. Photodyn. Ther., **8** (4), 337 (2011). DOI: 10.1016/j.pdpdt.2011.06.002
[6] C. Shirata, J. Kaneko, Y. Inagaki et. al. Sci. Rep., **7**, 13958 (2017). DOI: 10.1038/s41598-017-14401-0
[7] S. Li, S. Yang, C. Liu, J. He, T. Li, C. Fu, X. Meng, H. Shao. Int. J. Nanomedicine, **16**, 433 (2021). DOI: 10.2147/IJN.S275938
[8] A. Hackethal, M. Hirschburger, S. Eicker, et. al. Geburtshilfe und Frauenheilkunde, **78** (01), 54 (2018). DOI: 10.1055/s-0043-123937
[9] Y.-H. Han, Ranjith K. Kankala, Sh.-B. Wang, Ai-Zheng. Chen. Nanomaterials, **8** (6), 360 (2018). DOI: 10.3390/nano8060360
[10] G. Jo, B.Y. Lee, E.J. Kim, M.H. Park, H. Hyun. Biomedicines, **8** (11), 476 (2020). DOI: 10.3390/biomedicines8110476
[11] K. Gowsalya, V. Yasothamani, R. Vivek. Nanoscale Adv., **3**, 3332 (2021). DOI: 10.1039/D1NA00059D
[12] W. Li, H. Zhang, X. Guo, et al. ACS Appl. Mater Interfaces, **9**, 3354 (2017). DOI: 10.1021/acsami.6b13351
[13] R. Philip, A. Penzkofer, W. Bäiumler, R.M. Szeimies, C. Abels. J. Photochem. Photobiol. A, **96** (1–3), 137 (1996). DOI: 10.1016/1010-6030(95)04292-X
[14] S. Reindl, A. Penzkofer, S.H. Gong, M. Landthaler, R. Szeimies, C. Abels, W. Bumler. J. Photochem. Photobiol. A, **105** (1), 65 (1997). DOI: 10.1016/s1010-6030(96)04584-4
[15] A. Gerega, N. Zolek, T. Soltysinski, D. Milej, P. Sawosz, B. Toczylowska, A. Liebert. J. Biomed. Opt., **16** (6), 067010 (2011). DOI: 10.1117/1.3593386
[16] N.Y. Hong, H.R. Kim, H.M. Lee, D.S. Sohn, K.G. Kim. Biomed. Opt. Express, **7** (5), 1637 (2016). DOI: 10.1364/BOE.7.001637
[17] T. Jin, S. Tsuboi, A. Komatsuzaki, Y. Imamura, Y. Muranaka, T. Sakata, H. Yasuda. Med. Chem. Commun., **7**, 632 (2016). DOI: 10.1039/c5md00580a
[18] E.H. Lee, J.K. Kim, J.S. Lim, S.J. Lim. Colloids Surf. B, **136**, 305 (2015). DOI: 10.1016/j.colsurfb.2015.09.025
[19] A.K. Kirchherr, A. Briel, K. Mder. Mol. Pharm., **6** (2), 480 (2009). DOI: 10.1021/mp8001649
[20] B. Jung, V.I. Vullev, B. Anvari. IEEE J. Sel. Top. Quantum. Electron., **20** (2), 7000409 (2014). DOI: 10.1109/jstqe.2013.2278674
[21] E.I. Altınolu, T.J. Russin, J.M. Kaiser, B.M. Barth, P.C. Eklund, M. Kester, J.H. Adair. ACS Nano., **2** (10), 2075(2008). DOI: 10.1021/nn800448r
[22] C.H. Lee, S.H. Cheng, Y.J. Wang, Y.C. Chen, N.T. Chen, et. al. Adv. Funct. Mater., **19** (2), 215 (2009). DOI: 10.1002/adfm.200800753
[23] R.H. Patel, A.S. Wadajkar, N.L. Patel, V.C. Kavuri, K.T. Nguyen, H. Liu. J. Biomed. Opt., **17** (4), 046003 (2012). DOI: 10.1117/1.jbo.17.4.046003

[24] F.P. Navarro, M. Berger, S. Guillermet, V. Josserand, L. Guyon, E. Neumann, F. Vinet, I. Texier. J. Biomed. Nanotechnol., **8**, 730 (2012). DOI: 10.1166/jbn.2012.1430
[25] Z. Sheng, D. Hu, M. Zheng, P. Zhao, H. Liu, et. al. ACS Nano., **8**, 12310 (2014). DOI: 10.1021/nn5062386
[26] Q. Chen, C. Liang, X. Wang, J. He, Y. Li, Z. Liu. Biomaterials, **35**, 9355 (2014). DOI: 10.1016/j.biomaterials.2014.07.062
[27] P. Huang, Y. Gao, J. Lin, H. Hu, H. Liao, et. al. ACS Nano., **9**, 9517 (2015). DOI: 10.1021/acsnano.5b03874
[28] T.S. Kondratenko, M.S. Smirnov, O.V. Ovchinnikov, I.G. Grevtseva, A.N. Latyshev. Opt. Spectr., **128** (8), 1278 (2020). DOI: 10.1134/S0030400X20080172
[29] T.S. Kondratenko, M.S. Smirnov, O.V. Ovchinnikov, I.G. Grevtseva. J. Nanopart. Res., **22** (9), 271 (2020). DOI: 10.1007/s11051-020-04981-w
[30] T.S. Kondratenko, M.S. Smirnov, O.V. Ovchinnikov, I.G. Grevtseva. J. Fluoresc., **30** (3), 581 (2020). DOI: 10.1007/s10895-020-02521-2
[31] E.S. Tuchina, V.V. Tuchin, B.N. Khlebtsov, N.G. Khlebtsov. Quantum Elec., **41** (4), 354 (2011). DOI: 10.1070/QE2011v041n04ABEH014595
[32] R. Jijie, T. Dumych, L. Chengnang, J. Bouckaert, K. Turcheniuk, et. al. J. Mater. Chem. B, (2016). DOI: 10.1039/C5TB02697K
[33] J. Malicka, I. Gryczynski, C.D. Geddes, J.R. Lakowicz. J. Biomed. Opt., **8** (3), 472 (2003). DOI: 10.1117/1.1578643
[34] B. Zhang, L. Wei, Zh. Chu. J. Photochem. Photobiol. A: Chem., **375**, 244 (2019). DOI: 10.1016/j.jphotochem.2019.02.028
[35] Y. Liu, M. Xu, Q. Chen, G. Guan, W. Hu, X. Zhao, et. al. Int. J. Nanomedicine, 4747 (2015). DOI: 10.2147/IJN.S82940
[36] F. Tam, G.P. Goodrich, Br.R. Johnson, N.J. Halas. Nano Lett., **7** (2) 496 (2007). DOI: 10.1021/nl062901x
[37] N. Toropov, A. Kamalieva, R.O. Volkov, E. Kolesova. Optics & Laser Technology, **121**, 105821 (2020). DOI: 10.1016/j.optlastec.2019.105821
[38] Y. Luo, J. Zhao. Nano Research., **12** (9), 2164 (2019). DOI: 10.1007/s12274-019-2390-z
[39] I.G. Grevtseva, T.A. Chevychelova, V.N. Derepko, O.V. Ovchinnikov, M.S. Smirnov, A.S. Perepelitsa, A.S. Parshina. Kondensirovannye sredy i mezhfaznye granitsy, **23** (1), 25 (2021) (in Russian). DOI: 10.17308/kcmf.2021.23/3294
[I.G. Grevtseva, T.A. Chevychelova, V.N. Derepko, O.V. Ovchinnikov, M.S. Smirnov, A.S. Perepelitsa, A.S. Parshina. Condensed Matter and Interphases, **23** (1), 25 (2021). DOI: 10.17308/kcmf.2021.23/3294].
[40] I.G. Grevtseva, T.A. Chevychelova, V.N. Derepko, M.S. Smirnov, A.N. Latyshev, O.V. Ovchinnikov, E.I. Enikeev, P.A. Golovinski, A.S. Selyukov. Bulletin of the Lebedev Physics Institute, **48** (3), 81 (2021). DOI: 10.3103/S1068335621030052.
[41] V.V. Savchuk, R.V. Gamernyk, I.S. Virt, et. al. AIP Advances, **9**, 045021 (2019). DOI: 10.1063/1.5090900
[42] A.L. Rodarte, A.R. Tao. J. Phys. Chem. C, **121** (6), 3496 (2017). DOI: 10.1021/acs.jpcc.6b08905
[43] X. Meng, A.V. Kildishev, K. Fujita, et. al. Nano Lett., **13** (9), 4106−4112 (2013). DOI: 10.1021/nl4015827
[44] N. Toropov, A. Kamalieva, A. Starovoytov, S. Zaki, T. Vartanyan. Adv. Photonics Res., **2**, 2000083 (2021). DOI: 10.1002/adpr.202000083
[45] B.I. Shapiro, E.S. Kol'tsova, A.G. Vitukhnovskii, et. al. Nanotechnologies in Russia, **6**, 456 (2011). DOI: 10.1134/S1995078011040112
[46] A.N. Kamalieva, N.A. Toropov, K.V. Bogdanov, T.A. Vartanyan. Opt. Spectrosc., **124** (3), 319 (2018). DOI: 10.1134/S1995078011040112
[47] E.M. Purcell. Phys. Rev., **69**, 681 (1946). DOI: 10.1103/PhysRev.69.674.2
[48] J. Li, A. Krasavin, L. Webster, et al. Sci Rep., **6**, 21349 (2016). DOI: 10.1038/srep21349
[49] E. Tóth, D. Ungor, T. Novák, et. al. Nanomaterials, **10**, 1048 (2020). DOI: 10.3390/nano10061048
[50] R. Becker, B. Liedberg, P.-O. Käll. J. Colloid. Interf. Sci., **343** (1) 25 (2010). DOI: 10.1016/j.jcis.2009.10.075
[51] F.W.B. van Leeuwen, B. Cornelissen, F. Caobelli, et. al. EJNMMI Radiopharm. Chem., **2** (15), (2017). DOI: 0.1186/s41181-017-0034-8
[52] A.-K. Kirchherr, A. Briel, K. Mader. Mol. Pharm., **6** (2), 480 (2009). DOI: 10.1021/mp8001649
[53] M. Törnblom, U. Henriksson, M.J. Ginley. Phys. Chem. B, **101** (19) 3901 (1997). DOI: 10.1021/jp9708660
[54] S. Link, M.B. Mohamed, M.A. El-Sayed. Phys. Chem. B, **103** (16), 3073 (1999). DOI: 10.1021/jp990183f
[55] T.C. Barros, S.H. Toma, H.E. Toma, E.L. Bastos, M.S. Baptista. J. Phys. Org. Chem., **23**, 893 (2010). DOI: 10.1002/poc.1692
[56] J.R. Lombardi, R.L. Birke. J. Phys. Chem. C, **112**, 5605 (2008). DOI: 10.1021/jp800167v